Cell Reports, Volume *20*

Supplemental Information

Phospho-Rasputin Stabilization by Sec16 Is Required for Stress Granule Formation upon Amino Acid Starvation

Angelica Aguilera-Gomez, Margarita Zacharogianni, Marinke M. van Oorschot, Heide Genau, Rianne Grond, Tineke Veenendaal, Kristina S. Sinsimer, Elizabeth R. Gavis, Christian Behrends, and Catherine Rabouille

Aguilera-Gomez et al, Cell Reports, 2017

Supplementary experimental procedures

Anti Rin antibody

The rabbit polyclonal anti-Rin was generated as follows: The *rin* coding region was PCR amplified from cDNA clone LD31994 (Berkeley *Drosophila* Genome Project) to add an NdeI site at the ATG and a BamHI site immediately following the stop codon. The PCR product was digested with NdeI and BamHI and inserted into the corresponding sites of pET15b. $(His)_6$-Rin was expressed in *E. coli* BL21 cells and then resolved by SDS-PAGE. The band corresponding to $(His)_6$-Rin was excised from the gel and used as the antigen to generate polyclonal rabbit anti-serum. The specificity of the antiserum was tested by immunoblotting of wild-type or rin^2/Df ovary extract and ECL detection. Anti-Rin was used at 1:500. The blot was re-probed with anti-Khc (1:20,000; Cytoskeleton) as a loading control (Suppl. Fig. S2D)

PMT-DNA constructs and dsRNAs

All the primers used for generating the DNA constructs and RNAi probes are listed in the Table below.

sfGFP-F	ggccgcggatggtgagcaagggcgagga
sfGFP-R	gggtttaaacttacttgtacagctcgtccatg
pMT- Rin -V5-F	cagtggtaccatggtcatggatgcgacccaatcg
pMT- Rin-V5-R	gtcaccgcgggcgacgtccgtagttgccaccac
pMT-Rin-S142A-V5-F	gaggacgagcaggatggcgaggcgcgatcggagaacgatgaggag
pMT-Rin-S142A-V5-R	ctcctcatcgttctccgatcgcgcctcgccatcctgctcgtcctc
pMT-Rin-S142E-V5-F	gaggacgagcaggatggcgaggagcgatcggagaacgatgaggag
pMT-Rin-S142E-V5-R	ctcctcatcgttctccgatcgctcctcgccatcctgctcgtcctc
pMT-Rin-d493-581-RRM-F	ttcggtgataat cgtgtccgcaacgacatggtgccgcgc
pMT-Rin-d493-581-RRM-R	gttgcggacacgattatcaccgaactgctgcgtgttgct
SEC16-SRD-F	cagtggtaccatgctgcagcaacagacgcgccc
SEC16-SRD-R	gtcaccgcggaatggggctgccatacgtttgcg
CAAX-RAS-F	cagtaccggttccggactcagatctcgagctc
CAAX-RAS-R	cagtgtttaaacttacataattacacactttgtctttgacttctttttc
CAAX-RAS-Sec16-F	cagtactagtatgttgcacaataatgcgccctggc
CAAX-RAS-Sec16-R	gtcaccgcggttgctggtgttgctgctgcagcg
SEC16>NC1-F	cagtactagtatgcattcaaccactcagcaggagaagaa
SEC16>NC1-R	ccaccggtaatggggctgccatacgtttgc
SEC16>CT-F	gtcaccgcggaaatgagacacgattaatgagaatgggatcatg
SEC16>CT-R	cagtggtaccatggcgagtcctccgaatgccactag
dsGFP-F	gggtttaaacttacttgtacagctcgtccatg
dsGFP-R	ggccgcggatggtgagcaagggcgagga
dsRin-F	taatacgactcactatagggccagacagattttcatagtgcg
dsRin-R	taatacgactcactatagggtggccatcattggatagctc
dsSec16-F	taataccgactcactatagggcgagatatggagcatttgacggagg
dsSec16-R	taatacgactcactatagggcgacttttctcgtgtggatgtgtgtg

To generate pMT-Rin-V5, Rin was amplified from S2 cells DNA and cloned into pMT-V5 using *SacII* and *KpnI*. To generate the mutant pMT-RinS142A, Rin cross-was amplified using primers harbouring a mutation at position S142A and cloned into pMT-V5 using *SacII* and *KpnI*. To generate the mutant PMT-Rin S142E Rin was cross-amplified using primers harbouring a mutation at position S142A and cloned into pMT-V5 using *SacII* and *KpnI*.

To generate the pMT-CAAX-sfGFP vector, the sequence corresponding to C-terminus CAAX motif of Ras (SGLRSRAQASNSRVKMSKDGKKKKKKSKTKCVIM) was

amplified and cloned into pMT-sfGFP using *AgeI* and *PmeI*. The Sec16 truncations: ΔNC1, ΔCter; Cter, SRD and Fl were cloned into pMT-CAAX-sfGFP using *EcoI* and *ApaI*.

To generate the pMT-sfGFP vector, super folder (sf) GFP was amplified and cloned into pMT-V5 using *SacII* and *PmeI* restriction sites replacing the V5 tag with sfGFP.

To generate the pMT Sec16 SRDC-sfGFP vector, SRDC was amplified from pMT Sec16fl GFP and cloned into pMT-sfGFP using *SacII* and *PmeI* restriction sites .

To generate the PMT-Rin-V5 ΔRRM, Ran was amplified using primers harbouring the RRM deletion (493-581aa) and cloned into pMT-V5 using KpnI and SacII.

The dsRNAs used for RNAi of Rin and Sec16 were amplified using primers harbouring T7 promoters in their sequence and used for *in vitro* transcription using the T7 Megascript Kit (AMBION) to generate the dsRNAs in the Table above.

Immuno-precipitation and mass spectrometry (MS/MS)

Sec16 immuno-precipitation: 200-300 million S2 cells were grown and starved in KRB for 4h. Cell lysate was prepared by incubating cells for 20 min on ice in lysis buffer (10% glycerol, 1% TritonX-100, 50mM TrisHCl pH 7.5, 150mM NaCl, 50mM NaF, 25mM Na_2-glycerophosphate, 1mM Na_2VO_4, 5mM EDTA, tablet protease inhibtors tablet (Roche). Protein A beads slurry was washed with lysis buffer and incubated for 1 hour at 4^0C with 20 ug of control IgG and anti Sec16 IgG. Subsequently, the beads where incubated for 2 hours at 4^0C with cell lysate. After washing with lysis buffer, beads where boiled for 10 min in sample buffer followed by SDS-PAGE and Western blot was performed.

Mass spectrometry: Endogenous Sec16 was immunoprecipitated from growing and starved S2 cells as described above and separated by SDS-PAGE. In-gel-trypsin digestion of the immunoprecipitates was performed as described previously (Shevchenko et al., 2006). Briefly, each lane was cut into five pieces and each piece was dehydrated with acetonitrile, reduced with DTT, alkylated with iodoacetamide and digested overnight with trypsin. Tryptic peptides were extracted with acetonitrile, desalted and analyzed by liquid chromatography tandem mass spectrometry (LC-MS/MS) using an Orbitrap Elite mass spectrometer coupled to a EasyLC nano-HPLC system (both Thermo Fisher Scientific, Dreieich, Germany). Peptide mixtures were loaded on a C18 reverse phase column in Solvent A (0.5% acetic acid) and eluted with a 5%-33% gradient solvent B (80% acetonitril in 0.5% acetic acid) running at a constant flow rate of 200 nl/min. Full-scan MS spectra were acquired in a mass range from m/z 300 to 2,000 with a resolution of 120.000 without lock mass. The 20 most intense precursor ions were sequentially CID fragmented in each scan cycle. In all measurements, up to 500 sequenced precursor masses were excluded from further analysis for 90 s. The target values of the mass analyzers were 1 million charges (MS) and 5,000 charges (MS/MS). The MS data was processed using default parameters of the MaxQuant software (1.5.3.8) (Cox and Mann, 2008). The peak lists were queried against the *Drosophila* UniProt database (2012_12). Full tryptic specificity was required, and up to two missed cleavages were allowed. Carbamidomethylation of cysteine was set as fixed modification. Protein N-terminal acetylation and oxidation of methionine were set as variable modifications. Initial precursor mass tolerance was set to 20 ppm and 0.5 Da at the fragment ion level. False discovery rates were set to 1% at peptide and protein group level.

To be scored as Sec16-interacting proteins, candidates were required to 1) be present in at least 2 experiments (out of 4 biological replicates) with at least 2 peptides per experiment and experimental conditions (growing and/or starvation) and 2) have an intensity of $\log_2$ (IgG:SEC16) ≥ 1 or in cases were proteins were not found in IgG control, have an intensity > 0. See Suppl Table 2 reporting the frequency of identification and the growth conditions. Both categories are color-coded and sortable.

Legends for Supplementary Figures and Tables

Suppl. Figure S1: Stress granules form upon amino-acid starvation and are distinct from autophagosomes (Related to Figure 1)
A-B: IF visualisation of FMR1 in cells incubated in culture medium (A), and KRB (A') supplemented or not with dialysed fetal bovine serum (FBS). Quantified in B.
Note that the absence of FBS does not lead to stress granule formation in cells incubated in culture medium. Conversely, note that the presence of FBS does not prevent stress granule formation in cells incubated in KRB (similar to **(Damgaard and Lykke-Andersen, 2011)** for HeLa cells). This demonstrates that the trigger of stress granule formation is amino-acid starvation.
C: Visualisation of the autophagosome marker Atg5-GFP and FMR1 in cells incubated in Schneider's and KRB for 3h. Note that stress granules and autophagosomes form upon starvation, but that they do not co-localise.

Suppl. Figure S2: Description of Rin, its domain and the anti-Rin rabbit polyclonal antibody (Related to Figure 2).
A: Comparison of the domain organisation in Rin and G3BP**.**
B: Ser142 in Rin is equivalent to Ser149 in G3BP. Drosophila Rin protein was used in a protein Blast against the NCBI NR database limited to eukaryotic sequences. The resulting 1704 protein sequences were used to generate a multiple sequence alignment. This analysis clearly showed that Ser149 from human G3BP directly aligns with the Drosophila Ser142 and that they are conserved.
C: Identification of the Rin RRM domain. Within the same alignment as described in B, 4 stretches of amino-acids in the region between Q493 and P581 (red boxes) were found highly conserved and correspond to RRM domains experimentally validated in G3BP.
D: The specificity of the Rin antiserum was tested by Western blotting of wild-type and rin^2/Df ovary extract and ECL detection. Anti-Rin was used at 1:500,000. The blot was re-probed with anti-Khc (1:20,000; Cytoskeleton) as a loading control. Note that the band at 75Kd disappears in the mutant extract.

Suppl. Figure S3: **Characterisation of Sec16 interaction with Rin (**Related to Figure 3).
A: WB visualisation of FRM1 and Caprin after Sec16 IP (after stripping of the blot shown in Figure 3D). FMR1 and Caprin do not appear to co-immunoprecipitate with Sec16.
B, B': Confocal section visualizating Rin-V5 (green) and Sec16 (red) after 0, 1, 2 h of amino-acid starvation. Sec16 and Rin increasingly appear to be in close proximity and overlapping. This interaction reaches its maximum at 2 h. Arrows point at Sec16 that is close to Rin. Quantified in C'.
C: Projection of 3 confocal sections co-visualising ΔNC1Sec16-GFP-CAAX and endogenous Rin (red) upon amino-acid starvation (KRB). Note that Rin is recruited to the plasma membrane
D: IF Visualisation of Rin ΔRRM-V5 (green) and FMR1 (red) in cells upon amino-acid starvation (KRB). Note that ΔRRM-V5 is not recruited to stress granules and also largely prevents their formation (arrowhead), whereas stress granules form normally in non-transfected cells.

Suppl. Figure S4: stress granule formation in DTT and heat shock (Related to Figure 4)

A: IF visualization of endogenous FMR1 in mock- and Sec16 depleted cells upon heat shock (3h) and DTT (3h). Note that stress granules form as efficiently in mock and Sec16 depleted cells.
B: IF visualization of FMR1 in mock- and Sar1 depleted cells incubated in KRB for 4h. Note that stress granule formation is as efficient in both depletions. Note that the Sar1 depletion was evidenced by the typical enlargement of the ERES **(Ivan et al., 2008).**
C: IF visualization of FMR1 in cells treated or not with BFA. Note that stress granule formation is as efficient in treated and non-treated cells.
Scale bars: 10 µm

Suppl. Figure S5: Stress granules formation in Sec16 depleted cells (Related to Figure 5)
A: Rin PCR product in mock and Sec16 depleted cells in growing conditions (Sch) and upon amino-acid starvation (KRB). Note that the level is similar. H2A acts as the control mRNA.
B: IF visualisation of Rin-V5 (green) and FMR1 (red) in mock- and Sec16 depleted transfected cells incubated in KRB supplemented or not with MG132. Note that MG132 incubation rescues Rin-V5 level in Sec16 depleted cells as well as the formation of stress granule formation in transfected cells (Rin-V5 and FMR1 positive, arrow).

However, whereas stress granules form in non-transfected mock-depleted cells upon KRB (double arrows, as shown in Figure 5D), stress granules do not form in non-transfected Sec16 depleted cells, even in the presence of MG132 (arrowhead). This clearly shows that Sec16 is needed for stress granule formation, not only for Rin recruitment.

Cox, J., and Mann, M. (2008). MaxQuant enables high peptide identification rates, individualized p.p.b.-range mass accuracies and proteome-wide protein quantification. Nature biotechnology *26*, 1367-1372.
Damgaard, C.K., and Lykke-Andersen, J. (2011). Translational coregulation of 5'TOP mRNAs by TIA-1 and TIAR. Genes & development *25*, 2057-2068.
Ivan, V., de Voer, G., Xanthakis, D., Spoorendonk, K.M., Kondylis, V., and Rabouille, C. (2008). Drosophila Sec16 mediates the biogenesis of tER sites upstream of Sar1 through an arginine-rich motif. Molecular biology of the cell *19*, 4352-4365.
Shevchenko, A., Tomas, H., Havlis, J., Olsen, J.V., and Mann, M. (2006). In-gel digestion for mass spectrometric characterization of proteins and proteomes. Nature protocols *1*, 2856-2860.

Supplementary Figure S1: Aguilera-Gomez et al, 2017

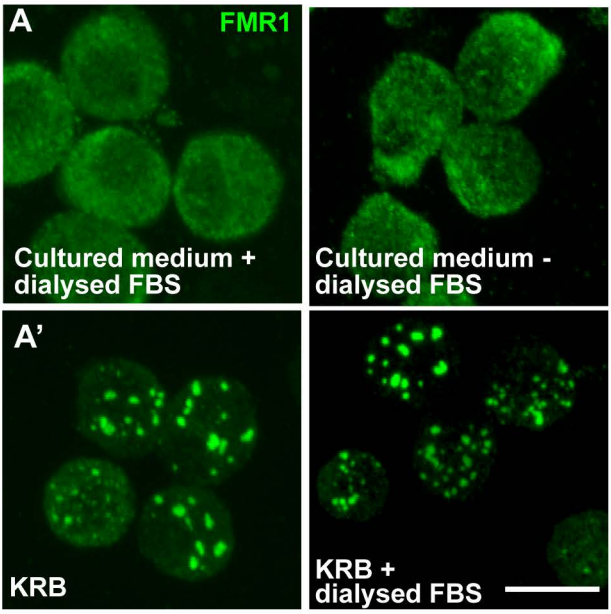

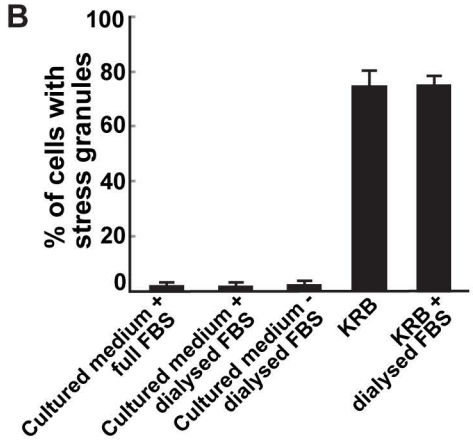

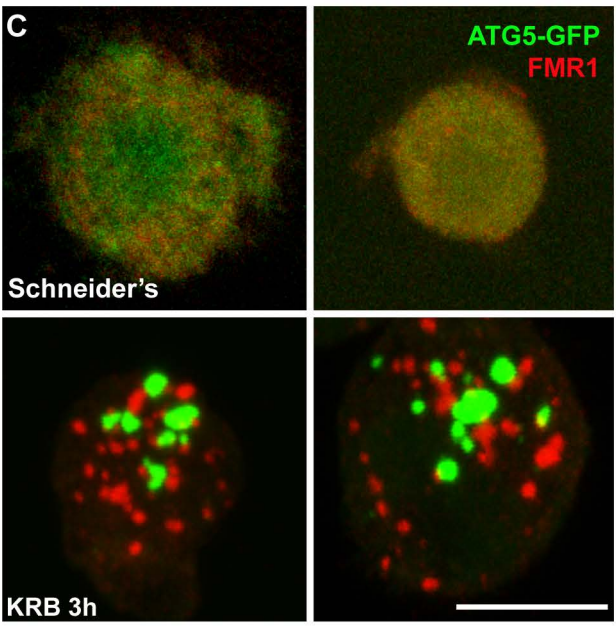

Supplementary Figure S2: Aguilera-Gomez et al, 2017

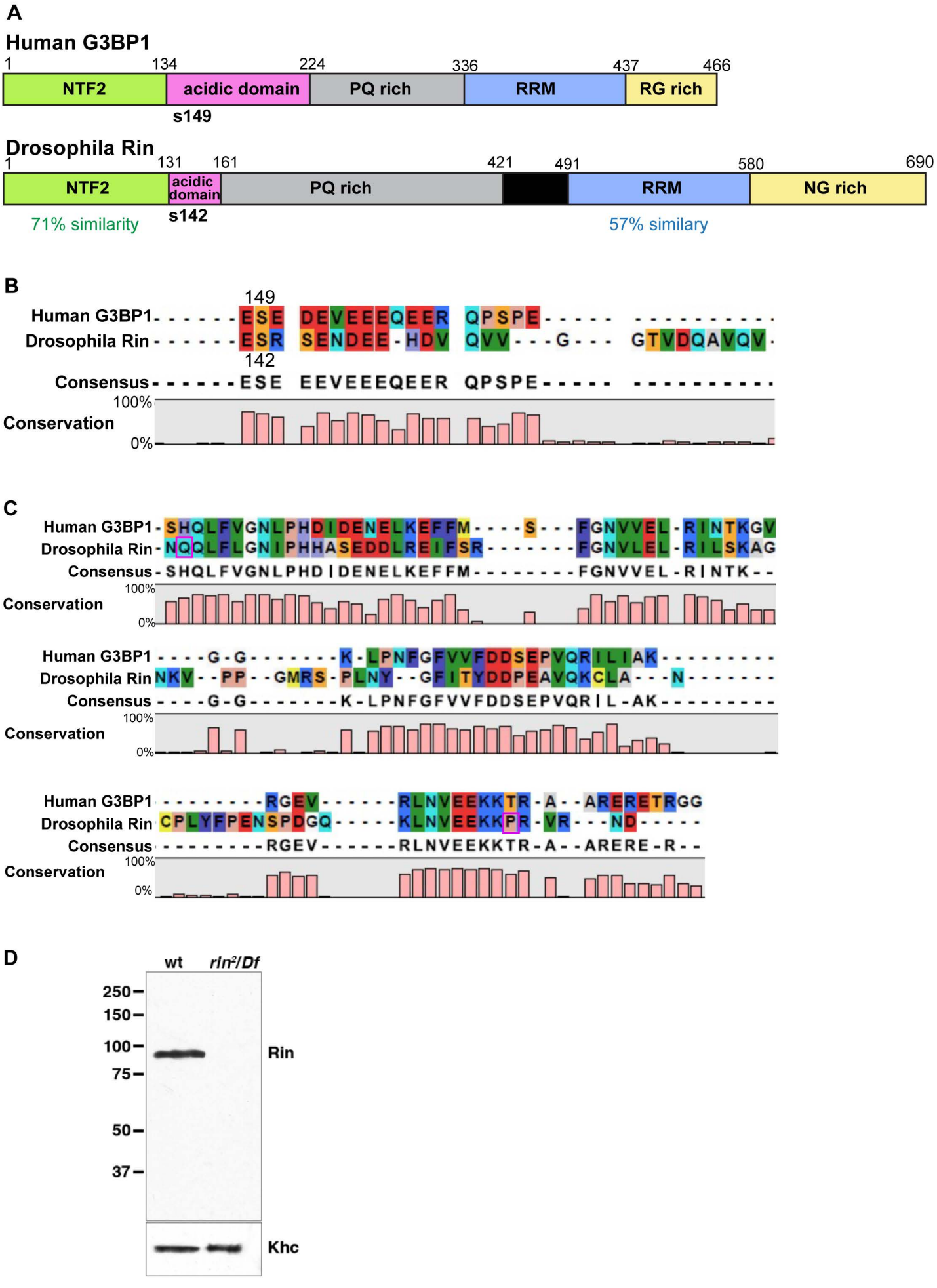

Supplementary Figure S3: Aguilera-Gomez et al, 2017

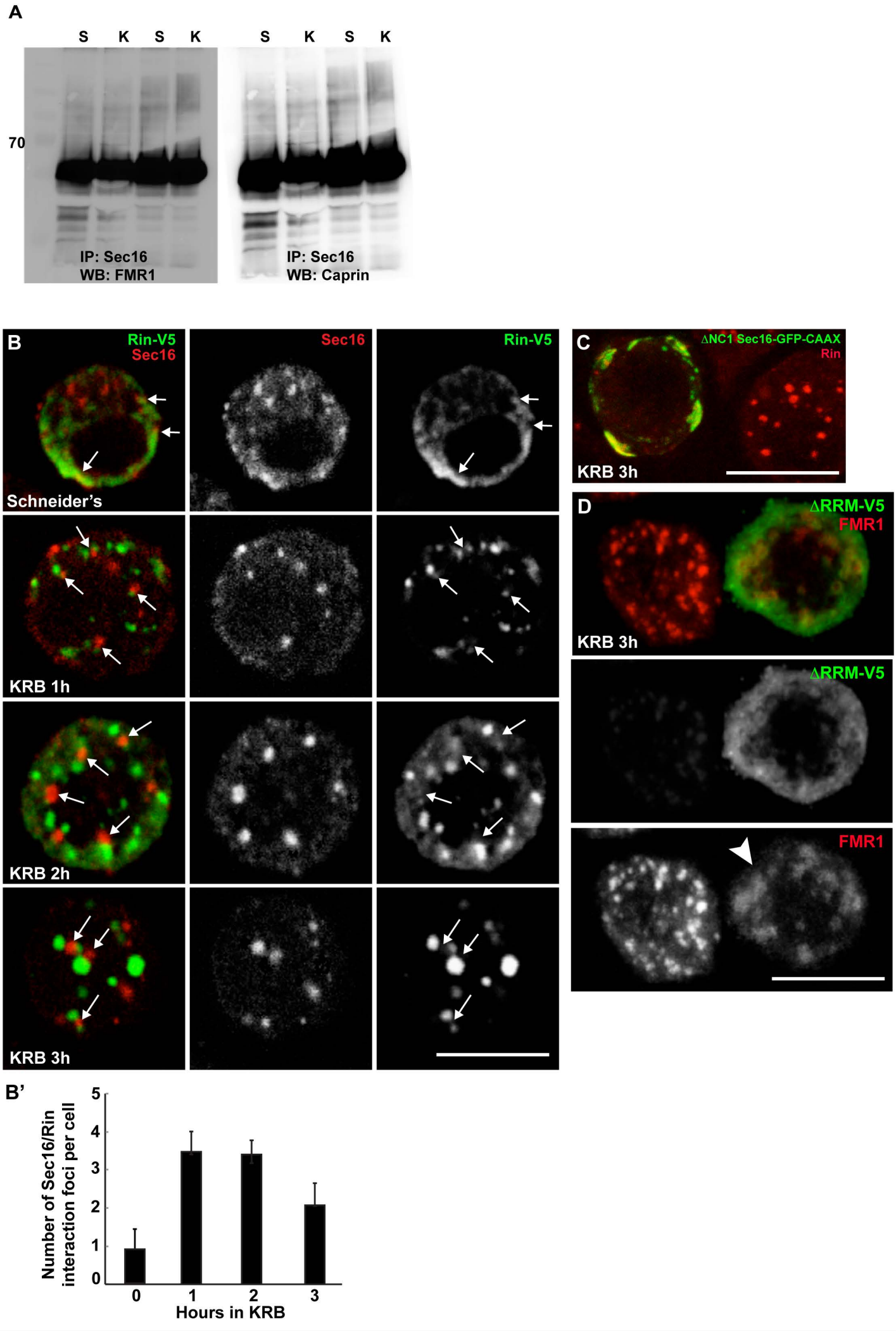

Supplementary Figure S4: Aguilera-Gomez et al, 2017

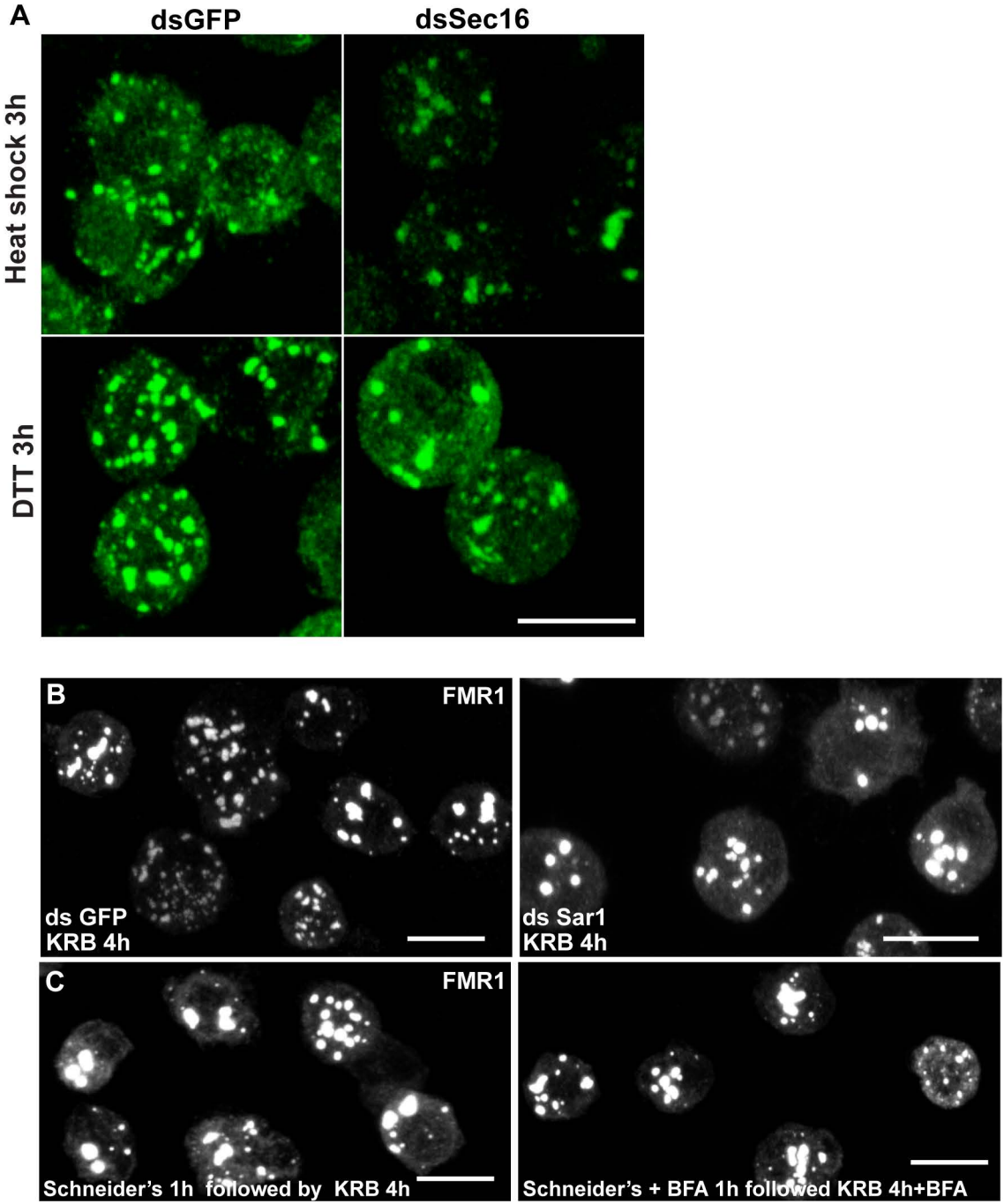

Supplementary Figure S5: Aguilera-Gomez et al, 2017

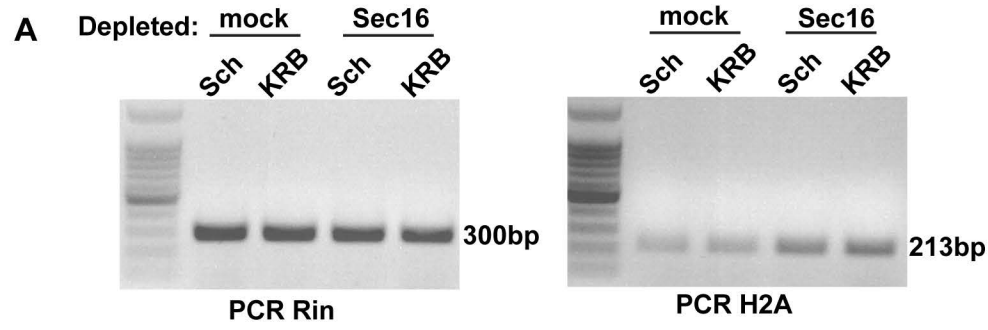

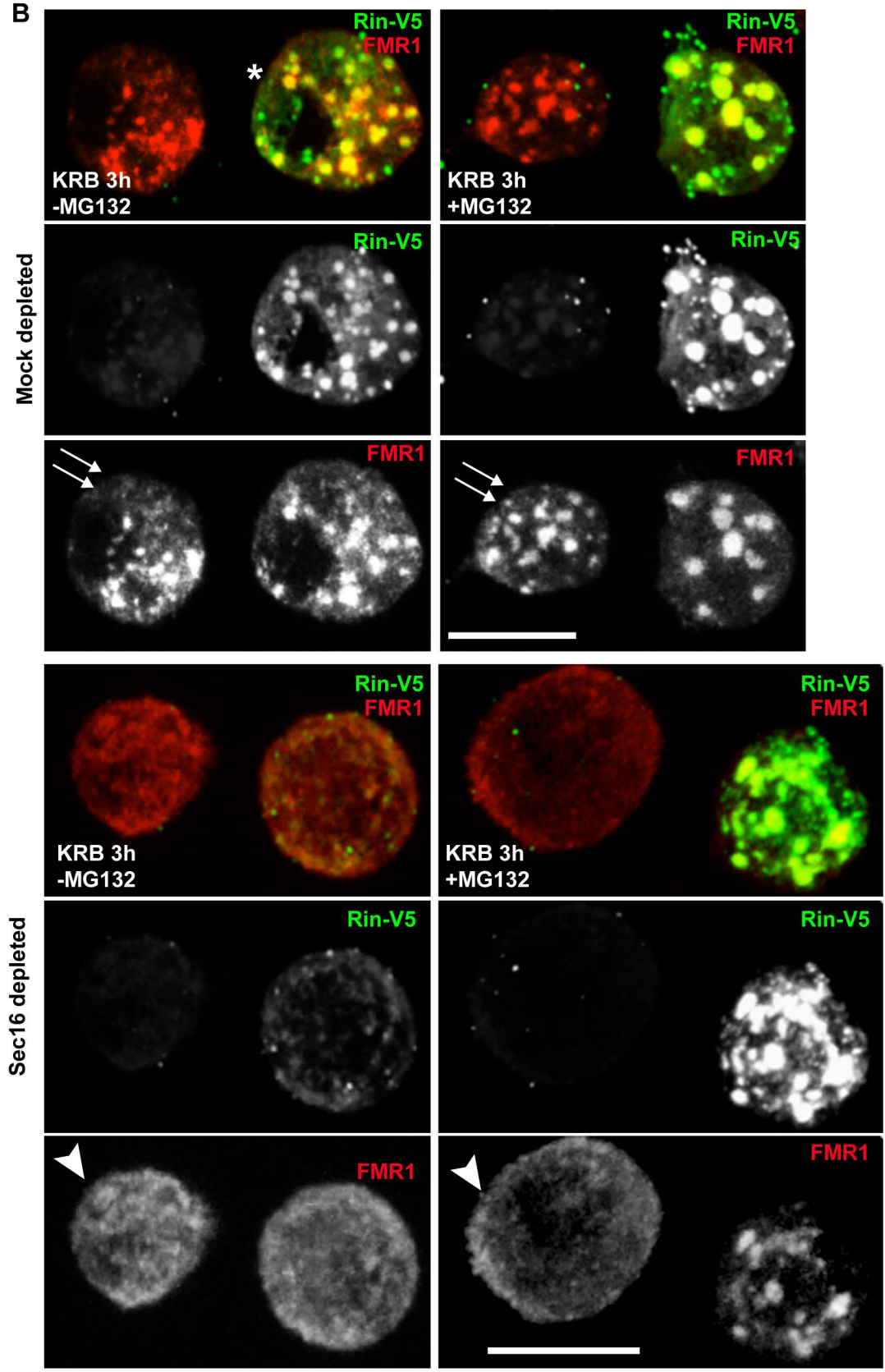

Supplementary Table S1

	Stress granules upon amino-acid starvation	Size	Number per cell
1	Endogenous	650±350 nm	11±6
2	Endogenous in S142A-V5 transfected cells	662 nm±100	29±5
3	Rin-V5 positive upon expression in wild type cells	751±120 nm	26±7
4	S142E-V5 positive upon expression in wild type cells	1000±60 nm	15±5
5	Rin-V5 positive upon expression in Rin depleted cells	630 nm	34±8
6	Reversion in full medium 3h	0	0
7	S142E-V5 positive upon expression in Rin depleted cells	1100±100 nm	17±4
8	Reversion in full medium 3h	640±90	33±6